

Free Vibration of Thin Axisymmetric Structures by a Semi-Analytical Finite Element Scheme and Isoparametric Solid Elements

T.A.I. Akeju

Department of Civil Engineering, University of Lagos, Lagos, Nigeria

D.W. Kelly, O.C. Zienkiewicz

*Department of Civil Engineering,
University of Wales, Singleton Park, Swansea, SA2 8PP, United Kingdom*

K. Kanaka Raju

Structural Engineering Division, Vikram Sarabhau Space Centre, Trivandrum, India

Abstract

The eigenvalue equations governing the free vibration of axisymmetric solids are derived by means of a semi-analytical finite element scheme. In particular we investigated the use of an 8-node solid element in structures which exhibit a "shell-like" behaviour. Bathe-Wilson subspace iteration algorithm is employed for the solution of the equations. The element is shown to give good results for beam and shell vibration problems. It is also utilised to solve a complex solid in the form of an internal component of a modern jet engine. This particular application is of considerable practical importance as the dynamics of such components form a dominant design constraint.

The work reported here was supported throughout by Rolls Royce (Jet Engine Division) who have a considerable wealth of experience in this type of analysis.

1. Introduction

The finite element method has received wide recognition for its immense capability to deal with two and three-dimensional problems. However, the cost of solution and the computer core required for the storage of the large matrices which are characteristic of such problems increase very rapidly with each additional dimension. Consequently a practical engineer is forced to search for alternatives which will reduce the computational cost.

A recourse is made in the present analysis to the fact that in many practical three-dimensional problems, the geometry and material properties do not vary along one particular coordinate direction.

The semi-analytical method considered is based on the fact that the shape function in that direction can be written in terms of Fourier series. The general formulation of the method can be found in reference [1]. For purposes of completeness we present a brief description of the formulation for dynamic problems in the next section and then proceed to actual derivation of the stiffness and mass matrices for the axisymmetric solid element.

Apart from the reduction in the dimensions of the problem, another merit of the method lies in the fact that certain definite integrals of products of the trigonometric terms in the Fourier series vanish, thereby uncoupling terms in the stiffness and mass matrices.

This analysis and the corresponding computer program were developed mainly for purposes of investigating the use of a solid element for problems which geometrically show a continuous variation from geometries calling for modelling by shell theories to those exhibiting full three-dimensional behaviour. In these cases neither model is optimal and an abrupt transition from one form of element to another would require some engineering judgement and therefore introduce a possible source of inaccuracy not necessarily removed by mesh refinement.

2. General Formulation

The general formulation given in [1] is briefly described here for dynamic problems.

Let (x, y, z) be the coordinates (not necessarily Cartesian) describing the domain of interest and consider one of these, z , as the coordinate along which the geometry and material properties do not vary and is limited to be between the two values,

$$0 \leq z \leq a.$$

The boundary values are thus prescribed at $z = 0$ and $z = a$.

We assume that the shape functions, defining the displacements, \bar{u} , are in the product form

$$\begin{aligned} \bar{u}(x, y, z) &= N(x, y, z) \bar{a}^e \\ &= \sum_{\ell=0}^L \{ \bar{N}(x, y) \cos \frac{\ell \pi z}{a} + \bar{\bar{N}}(x, y) \sin \frac{\ell \pi z}{a} \} \bar{a}^e \end{aligned} \quad (1)$$

Following standard finite element displacement formulation, a typical stiffness sub-matrix for two harmonics, ℓ, m and two nodes, i, j can be written as

$$(K_{ij}^{\ell m})^e = \iiint_V B_i^{\ell} D B_j^m dx dy dz \quad (2)$$

where within the finite element approximation and by standard notation

$$\epsilon = Bu \quad (3)$$

and

$$\sigma = D\epsilon \quad (4)$$

B and D are respectively the strain-displacement and stress-strain matrices.

It is obvious that the equation (2) derived by means of energy principles with equation (1) substituted for displacements, contains the products of various submatrices along with the integrals of the form

$$I_1 = \int_0^a \sin \frac{\ell\pi z}{a} \cos \frac{m\pi z}{a} dz$$

$$I_2 = \int_0^a \sin \frac{\ell\pi z}{a} \sin \frac{m\pi z}{a} dz \quad (5)$$

$$I_3 = \int_0^a \cos \frac{\ell\pi z}{a} \cos \frac{m\pi z}{a} dz$$

and due to the well known orthogonality property, the integrals I_2, I_3 are

$$I_2 = I_3 = 0 \text{ for } \ell \neq m. \quad (6)$$

Further I_1 is zero when ℓ and m are both even or odd numbers. The terms involving I_1 also vanish in most applications. This means that the matrix $(K)^e$ becomes a diagonal one and the assembled stiffness matrix will be of the form

$$\begin{bmatrix} K^{11} \\ K^{22} \\ \cdot \\ \cdot \\ \cdot \\ \cdot \\ K^{LL} \end{bmatrix}$$

where

$$K_{ij}^{\ell\ell} = \frac{a}{2} \iint B_i^{\ell T} D B_j^{\ell} dx dy \quad (7)$$

A similar approach yields the mass matrix also in the form

$$\begin{bmatrix} M^{11} \\ M^{22} \\ \cdot \\ \cdot \\ \cdot \\ \cdot \\ M^{LL} \end{bmatrix}$$

where

$$M_{ij}^{\ell\ell} = \frac{a}{2} \iint N_i^{\ell T} \rho N_j^{\ell} dx dy \quad (8)$$

ρ is the density matrix and N_i are the shape function matrices. It can easily be seen that this diagonal structure of the stiffness and mass matrices uncouples the large system of eigenvalue equation governing the vibration problem

$$[\mathbf{K}] \{\delta\} - \omega^2 [\mathbf{M}] \{\delta\} = 0 \quad (9)$$

into L separate eigenvalue equations

$$[\mathbf{K}^{\ell\ell}] \{\delta^{\ell\ell}\} - \omega_{\ell}^2 [\mathbf{M}^{\ell\ell}] \{\delta^{\ell\ell}\} = 0 \quad (10)$$

and thus allows for a separate solution for each harmonic. This indeed is an added advantage of the present semi-analytical method; for not only does it reduce the computational labour, it also leads to a great reduction of the computer core required for the storage of the stiffness and mass matrices.

3. Derivation of Stiffness and Mass Matrices

The general formulation described in the last section is now used to study the vibration characteristics of a few structural components. For convenience in describing the axisymmetric geometry considered, the cylindrical polar coordinates (r, θ, z) is used.

For a particular harmonic ℓ , the displacement components can be represented in the following forms

$$\begin{aligned} u^{\ell} &= \sum_{i=1}^n N_i(r, z) u_i^{\ell} \cos \ell \theta \cos \omega t \\ v^{\ell} &= \sum_{i=1}^n N_i(r, z) v_i^{\ell} \cos \ell \theta \cos \omega t \\ w^{\ell} &= \sum_{i=1}^n N_i(r, z) w_i^{\ell} \sin \ell \theta \cos \omega t \end{aligned} \quad (11)$$

where n is the number of nodes appropriate to the finite element idealisation scheme and w the displacement in the circumferential direction θ

The three-dimensional strain-displacement relations in polar coordinates are

$$\{\epsilon\} = \begin{Bmatrix} \epsilon_r \\ \epsilon_z \\ \epsilon_{\theta} \\ \gamma_{rz} \\ \gamma_{r\theta} \\ \gamma_{z\theta} \end{Bmatrix} = \begin{Bmatrix} \frac{\partial u}{\partial r} \\ \frac{\partial v}{\partial z} \\ \frac{u}{r} + \frac{1}{r} \frac{\partial w}{\partial \theta} \\ \frac{\partial u}{\partial z} + \frac{\partial v}{\partial r} \\ \frac{1}{r} \frac{\partial u}{\partial \theta} + \frac{\partial w}{\partial r} - \frac{w}{r} \\ \frac{1}{r} \frac{\partial v}{\partial \theta} + \frac{\partial w}{\partial z} \end{Bmatrix} \quad (12)$$

and can be written in the familiar finite element form as

$$\{\epsilon\} = [\mathbf{B}] \{u\} \quad (3)$$

in which $\{u\}$ is the vector of nodal displacements and the B matrix for the i th mode is

$$B_i^{\ell} = \begin{bmatrix} \frac{\partial N_i}{\partial r} \cos l\theta & 0 & 0 \\ 0 & \frac{\partial N_i}{\partial z} \cos l\theta & 0 \\ \frac{N_i}{r} \cos l\theta & 0 & \frac{l N_i}{r} \cos l\theta \\ \frac{\partial N_i}{\partial z} \cos l\theta & \frac{\partial N_i}{\partial r} \cos l\theta & 0 \\ -\frac{l N_i}{r} \sin l\theta & 0 & \left(\frac{\partial N_i}{\partial r} - \frac{N_i}{r}\right) \sin l\theta \\ 0 & -\frac{l N_i}{r} \sin l\theta & \frac{\partial N_i}{\partial z} \sin l\theta \end{bmatrix} \quad (13)$$

The last expression can be conveniently separated into two as follows:

$$B_i^{\ell} = [B_i^{\ell}] \sin l\theta + [\bar{B}_i^{\ell}] \cos l\theta \quad (14)$$

where

$$B_i^{\ell} = \begin{bmatrix} 0 & 0 & 0 \\ 0 & 0 & 0 \\ 0 & 0 & 0 \\ 0 & 0 & 0 \\ \frac{l N_i}{r} & 0 & \left(\frac{\partial N_i}{\partial r} - \frac{N_i}{r}\right) \\ 0 & -\frac{l N_i}{r} & \frac{\partial N_i}{\partial z} \end{bmatrix}; \quad \bar{B}_i^{\ell} = \begin{bmatrix} \frac{\partial N_i}{\partial r} & 0 & 0 \\ 0 & \frac{\partial N_i}{\partial z} & 0 \\ \frac{N_i}{r} & 0 & \frac{l N_i}{r} \\ \frac{\partial N_i}{\partial z} & \frac{\partial N_i}{\partial r} & 0 \\ 0 & 0 & 0 \\ 0 & 0 & 0 \end{bmatrix} \quad (15)$$

The element stiffness matrix is therefore given by

$$[K_{ij}^{\ell}]^e = \iiint [B_i^{\ell}]^T D [B_j^{\ell}] r dr d\theta dz \quad (16)$$

where D, the three-dimensional elasticity matrix is given by

$$D = \begin{bmatrix} 1 & \frac{\nu}{1-\nu} & \frac{\nu}{1-\nu} & 0 & 0 & 0 \\ & 1 & \frac{\nu}{1-\nu} & 0 & 0 & 0 \\ & & 1 & 0 & 0 & 0 \\ & & & \frac{1-2\nu}{2(1-\nu)} & 0 & 0 \\ \text{Symmetric} & & & & \frac{1-2\nu}{2(1-\nu)} & 0 \\ & & & & & \frac{1-2\nu}{2(1-\nu)} \end{bmatrix} \quad (17)$$

Substituting (14) in (16) and noting that

$$\int_0^{2\pi} \sin l\theta \sin m\theta d\theta = \int_0^{2\pi} \cos l\theta \cos m\theta d\theta = 0 \text{ if } l \neq m \\ = \pi \text{ if } l = m > 0 \quad (18)$$

the element stiffness matrix reduces to

$$[K_{ij}^{\ell}]^e = \pi \iint \{ [B_i^{\ell}]^T D_{11} [B_j^{\ell}] + [\bar{B}_i^{\ell}]^T D_{22} [\bar{B}_j^{\ell}] \} r dr dz \quad (19)$$

where D_{11} , D_{22} are the partitioned D matrices.

Similarly equation (18) can be used to show that the element mass matrix reduces to

$$[M_{ij}^{\ell\ell}]^e = \pi \iint \begin{bmatrix} \rho N_i N_j & 0 & 0 \\ 0 & \rho N_i N_j & 0 \\ 0 & 0 & \rho N_i N_j \end{bmatrix} r dr dz \quad (20)$$

where ρ is the mass density. For $\ell = m = 0$ the integrals (19) and (20) maintain their respective values except for a scaling factor of 2π rather than π .

Assembling the equations by well known standard finite elements procedure leads to the eigenvalue problem of equation (9); i.e.

$$[K] \{\delta\} - \omega^2 [M] \{\delta\} = 0 \quad (9)$$

where K is the assembled stiffness matrix, M is the assembled mass matrix and ω are the frequencies corresponding to the assumed mode (11).

Equation (9) can be solved conveniently by any of the methods for solving standard eigenvalue problem posed by large symmetric banded matrix as for example used in this case the Bathe-Wilson subspace iteration algorithm [2].

4. Numerical Application

The accuracy and convergence characteristics of the finite element scheme described above were tested by using it to determine the natural frequencies of a cylindrical shell (Figure 1), which has been used in the past [3, 4] to check shell vibration analysis. It was also applied to vibrations of a cantilever shaft for which analytical solutions exist [5].

All the results were produced using the eight-noded two-dimensional isoparametric element [1]. Both consistent and lumped mass schemes are used. Mass lumping was effected by scaling the diagonal terms of the consistent mass matrix to preserve the total mass of the system and off diagonal terms are set to zero. Where appropriate comparison of lumped mass and consistent mass results are given and the type of mass matrix is identified.

The shaft problem was solved for a single row of four, eight and sixteen elements respectively and the first three modes in the zeroth and first harmonic compared with analytical solutions in Table 1.

The comparable analytical solutions [5] for the shaft problem are for the first and third mode of the zeroth harmonic represented by the first two torsional vibration modes of a cantilever shaft whilst the second mode is comparable to the longitudinal vibration mode of a rod. The first harmonic solutions correspond to those of a Eulerian cantilever beam.

Despite the fairly large aspect ratio of the elements used to model the shaft and the inclusion of in-plane inertia effects in the numerical model, close agreement with analytical solutions are observed in the results of Table 1.

The cylindrical shell (Figure 1) was modelled with fifteen elements in a row along the length so as to produce an aspect ratio of about 15 for each of the elements. The results given in Table 2 compared favourably with those of published high precision shell element solutions [3] and finite difference solutions [4].

As a final example, we consider a component of a modern jet engine for which some experimental results have been made available. Finite element discretizations are given in

Figure 2.

In Table 3, we present the finite element results for two different meshes alongside those determined experimentally by the Rolls Royce Company Limited. The first eight natural frequencies were determined using a mesh of 77 elements (Figure 2) and lumped mass scheme. The same mesh was also used to determine a few of the lowest natural frequencies with consistent mass scheme.

Solution for a refined mesh with 187 elements (Figure 2) was only possible for mass lumping scheme because of core limitation. The refined mesh results were as expected closer to the experimental results and an indication that further refinement will give accurate results. The implementation of reduced integration indicates the stiffening effect of the spurious shear term in this problem [6].

5. Conclusion

A semi-analytical finite element scheme for the analysis of complex three-dimensional axisymmetric solids has been utilised successfully to solve beam vibration problems and a cylindrical shell vibration problem.

The merit of this approach is the substantial reduction in the size of the three-dimensional problem. In geometries which combine shell-like behaviour connected to components of a true three-dimensional solid, the removal of the need for extra physical modelling approximation is significant. However, the practical value of the approach must depend on the accuracy of the solution of complex problems and in this context the results for the jet engine component presented here are encouraging.

Acknowledgement

The authors wish to thank the Rolls Royce Company Limited (Aero Division, Derby, U.K.) for providing the experimental data quoted in Table 3 and suggesting the solution of this problem. Financial support and several theoretical and technical discussions are also gratefully acknowledged.

References

- [1] ZIENKIEWICZ, O.C., "The Finite Element Method", McGraw Hill, London, (1977).
- [2] BATHE, K.J. and WILSON, E.L., "Numerical Methods in Finite Element Analysis", Prentice-Hall, New York, (1976).
- [3] SEN, S.K. and GOULD, P.L., "Free Vibration of Shells of Revolution using Finite Element Method", J. of Eng. Mech. Div. ASCE Vol. 100, No. EM2, pp 283-303, (April 1974).
- [4] AKEJU, T.A.I. and MUNRO, J., "Free Vibration of Shells of Revolution", Bulletin of International Association for Shells and Spatial Structures, Vol. 20, pp 9-28, (December 1974).
- [5] THOMSON, W.T., "Vibration Theory and Applications", Prentice-Hall, (1965).
- [6] ZIENKIEWICZ, O.C., TAYLOR, R.L. and TOO, J.M., "Reduced Integration Technique in General Analysis of Plates and Shells", Int. J. Num. Meth. Engrg. Vol. 3, pp 275-290, (1971).

TABLE 1
 NATURAL FREQUENCIES OF CIRCULAR SHAFT IN RADIANS/SEC

($E = 10^7$, $\nu = 0.3$, $\rho = 1.0$, $L/D = 20$)
 (3 x 3 integration)

| λ | Mode | 4 Elements Consistent Mass | 8 Elements Consistent Mass | 16 Elements Consistent Mass | Analytical |
|-----------|------|-------------------------------|-------------------------------|--------------------------------|------------|
| 0 | 1 | 51.3439 | 51.3431 | 51.3431 | 51.3431 |
| | 2 | 154.2247 | 154.0292 | 154.0313 | 154.0292 |
| | 3 | 251.3033 | 256.8731 | 256.7474 | 256.7154 |
| 1 | 1 | 2.3747 | 2.3388 | 2.3310 | 2.3190 |
| | 2 | 15.5350 | 14.6261 | 14.5025 | 14.5201 |
| | 3 | 47.4543 | 40.8922 | 40.1945 | 40.6484 |

TABLE 2
 NATURAL FREQUENCIES OF CYLINDRICAL SHELL (FIGURE 1)
 IN HERTZ

($E = 3.0 \times 10^7$ lb in⁻², $\nu = 0.3$, $\rho = 7.38 \times 10^{-4}$ lb in⁻⁴ sec²)
 (3 x 3 integration)

| λ | Mode | Present Work Consistent Mass | Reference 4 | Reference 5 |
|-----------|------|---------------------------------|-------------|-------------|
| 0 | 1 | 5480 | 5486 | 5483 |
| | 2 | 7881 | 8055 | 7653 |
| | 3 | 7942 | 8123 | 8018 |
| 1 | 1 | 2036 | 2033 | 2033 |
| | 2 | 5396 | 5431 | 5412 |
| | 3 | 6912 | 6986 | 6945 |

TABLE 3
 NATURAL FREQUENCIES OF JET ENGINE COMPONENT (cycles/sec.)

| Mode No. | 77 ELEMENTS | | | | | | 187 Elements | | Experimental (engine mass 898) $\lambda = 1$ |
|------------------|---------------|---------------|---------------|-----------------|---------------|---------------|---------------|-----|--|
| | LUMPED MASS | | | CONSISTENT MASS | | | LUMPED MASS | | |
| | $\lambda = 0$ | $\lambda = 1$ | $\lambda = 2$ | $\lambda = 0$ | $\lambda = 1$ | $\lambda = 0$ | $\lambda = 1$ | | |
| Integration Rule | 3 x 3 | 3 x 3 | 3 x 3 | 3 x 3 | 3 x 3 | 3 x 3 | 2 x 2 | | |
| 1 | 0 | 0 | | 0 | 0 | 0 | 0 | | |
| 2 | 0 | 0 | | 0 | 0 | 0 | 0 | | |
| 3 | 318.2 | 266.0 | > 860 | 320.2 | 268.4 | 245.0 | 242.3 | 247 | |
| 4 | 351.4 | 394.1 | | 359.7 | 398.5 | 339.9 | 334.3 | 323 | |
| 5 | 386.2 | 494.3 | | 388.2 | 504.2 | 420.5 | 412.5 | 386 | |
| 6 | 389.0 | 637.7 | | 397.3 | 650.1 | 429.7 | 421.2 | 411 | |
| 7 | 493.8 | 680.8 | | | | 479.0 | 469.4 | 453 | |
| 8 | 644.8 | 768.3 | | | | 604.3 | 598.2 | 585 | |

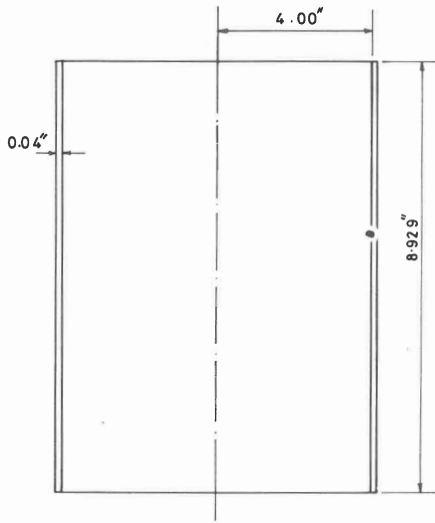


FIG.1. CYLINDRICAL SHELL

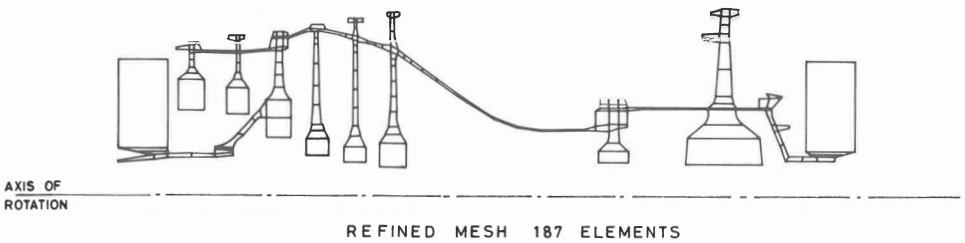
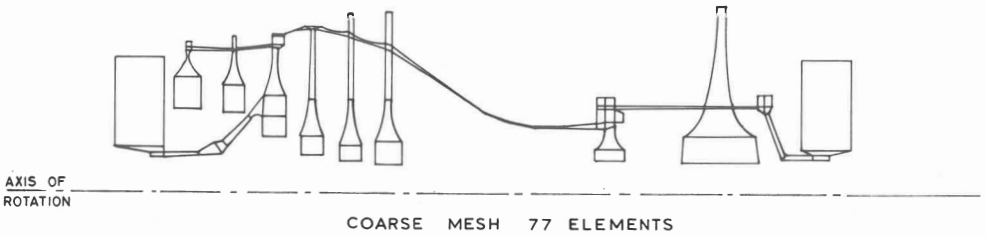


FIG. 2 COMPONENT OF A MODERN JET ENGINE

